



1 **Theoretical insights from upscaling Michaelis-Menten microbial**
2 **dynamics in biogeochemical models: a dimensionless approach**

3

4 Chris H. Wilson¹, Stefan Gerber²

5 ¹Agronomy Department, University of Florida, Gainesville, FL, USA 32611

6 ²Soil and Water Sciences Department, University of Florida, Gainesville, FL, USA 32611

7

8 *Correspondence to:* Chris H. Wilson (chwilson@ufl.edu)

9

10

11

12

13

14

15

16

17

18



19 **Abstract.** Leading an effective response to the accelerating crisis of anthropogenic climate
20 change will require improved understanding of global carbon cycling. A critical source of
21 uncertainty in Earth Systems Models (ESMs) is the role of microbes in mediating both the
22 formation and decomposition of soil organic matter, and hence in determining patterns of CO₂
23 efflux. Traditionally, ESMs model carbon turnover as a first order process impacted primarily by
24 abiotic factors, whereas contemporary biogeochemical models often explicitly represent the
25 microbial biomass and enzyme pools as the active agents of decomposition. However, the
26 combination of non-linear microbial kinetics and ecological heterogeneity across space
27 guarantees that upscaled dynamics will violate mean-field assumptions via Jensen's Inequality.
28 Violations of mean-field assumptions mean that parameter estimates from models fit to upscaled
29 data (e.g. eddy covariance towers) are likely systematically biased. Here we present a generic
30 mathematical analysis of upscaling michaelis-menten kinetics under heterogeneity, and provide
31 solutions in dimensionless form. We illustrate how out dimensionless form facilitates qualitative
32 insight into the significance of this scale transition, and argue that it will facilitate cross site
33 intercomparisons of flux data. We also identify the critical terms that need to be constrained in
34 order to unbiased parameter estimates.

35 1 Introduction

36 The current crisis of anthropogenic climate change is expected to accelerate during the 21st
37 century. Despite considerable effort to better constrain global biogeochemical models,
38 considerable uncertainty remains about how best to represent emerging mechanistic
39 understanding of soil element cycling into process-based models (Wieder et al. 2015, 2018;
40 Todd-Brown, Zheng, and Crowther 2018). This is a critical gap in knowledge because variations
41 among models predict hugely varying responses to global change drivers such as temperature,
42 soil moisture, and CO₂ enrichment. For example, a traditional first-order linear model forecasts
43 no change or even slight enhancement of soil organic carbon (SOC) pools by 2100 whereas one
44 microbial-explicit model forecasts a loss of ~70Pg of carbon (C), depending on whether
45 microbial physiology acclimates to higher temperatures (Wieder, Bonan, and Allison 2013). In
46 general, our understanding of how carbon (and other elements) cycles in soil is undergoing
47 significant revision toward a more microbial-centric paradigm. In contrast to traditional first-
48 order linear models (e.g. CENTURY, Parton et al. 1987), microbial explicit models feature non-
49 linear dynamics in which microbial biomass (or, similarly, microbially-driven enzyme pools) are
50 responsible for decomposition, in addition to providing substrate for synthesis of potentially
51 long-term SOC (Blankinship and Schimel 2018; Blankinship et al. 2018). While indisputably a
52 better representation of our scientific knowledge, non-linear microbial models face several well-
53 known challenges, including less analytical tractability, greater computational challenges, and
54 uncertainty about structural formulation and dynamics (Georgiou et al. 2017; Sihi et al. 2016).
55 However, one critical consequence of non-linear microbial models that is only recently gaining
56 attention is their implications for addressing the upscaling challenge.

57 While the fields of population and community ecology have long confronted the challenges
58 posed by non-linearity and heterogeneity in spatiotemporal scaling of ecological dynamics
59 (Chesson 2009; Levin 1992), ecosystem ecology and biogeochemistry have tended to approach
60 the challenge of scale either by 1) utilizing mean-field assumptions, or 2) addressing the
61 challenge of scaling via grid-based computational/numeric methods. While there is nothing



62 wrong inherently with either approach, they unfortunately cannot yield theoretical insight into
63 the consequences of non-linearity and heterogeneity for scaling. Briefly, the combination of non-
64 linearity and heterogeneity means that aggregated behavior differs systematically from mean-
65 field predictions, a special case of Jensen's Inequality. In mathematical notation:

$$66 \quad E[f(x)] \neq f(E[x]) \quad (1)$$

67 Although Jensen's Inequality is well-known from basic probability theory (Ross 2002), it's
68 implications for ecological dynamics under heterogeneity were not well-appreciated until the
69 pioneering work of Peter Chesson in the 1990s (Chesson 1998). In the case of carbon cycle
70 science, there are a few immediate and critical applications. For instance, most trace gas
71 emission processes are well-known to be non-linear functions of underlying drivers such as
72 temperature and soil moisture. For example, ecosystem respiration (hereafter " R_{eco} ") is an
73 exponential function of temperature (usually expressed in Q_{10}), and a unimodal function of soil
74 moisture. Thus, when matching observations of CO_2 efflux (" F ") to ecosystems, variations in
75 soil temperature and moisture could imply that F differs systematically from a mean-field
76 prediction. In addition to missing critical analytical insight, not accounting for this behavior
77 might have severe consequences for inverse modeling and estimation of the parameters
78 governing process-based models (PBMs). The basic consequences of Jensen's Inequality for
79 estimation of trace gas emission (CH_4 and N_2O) were first discussed by Van Oijen et al. (2017),
80 but have not been picked up on elsewhere, until the present work and by Chakrawal et al. (2019).

81 Chakrawal et al. (2019) provide a detailed and compelling first-pass application of scale
82 transition theory to biogeochemical modeling. Our contribution here complements their laudable
83 effort by providing a more generic mathematical analysis of the scale transition, equally
84 applicable to both forward and reverse michaelis-menten microbial kinetics. As in Chakrawal et
85 al. (2019), we address the consequences of heterogeneity in both substrate/microbes
86 ("biochemical heterogeneity") as well as in the kinetic parameters ("ecological heterogeneity").
87 However, we diverge from their approach in that, rather than explore detailed simulation models,
88 we derive a completely non-dimensionalized expression for aggregating non-linear microbial
89 kinetics over both types of heterogeneity simultaneously. We illustrate the enormous clarity this
90 brings in several special cases of our full analysis. Altogether, our approach provides universal
91 insight into the properties of the scale transition, and enables clear conclusions to be drawn
92 across systems in terms of the role of spatial variances and covariances in shaping ecosystem
93 carbon efflux. Our work provides a simplified, yet systematic framework around which to base
94 subsequent empirical and simulation-based studies.

95 **2. Carbon Efflux and the Scale Transition**

96 A variety of microbial-explicit PBMs have been proposed in the literature, starting with the
97 classic enzyme pool model of Schimel and Weintraub (2003). In order to elucidate universal
98 properties of the scale transition, we focus here on the CO_2 efflux following decomposition of a
99 single substrate by a single microbial pool obeying Michaelis-Menten (MM) dynamics:

$$100 \quad F = -f(C, MB, \theta) \quad (2)$$

101



102 where F is the CO_2 flux, θ is a vector of parameters, specifically V_{max} (the maximum reaction
103 rate given saturation of either C, in forward MM, or microbial biomass (MB), in reverse MM),
104 k_h (the half-saturation constant), and $1 - \epsilon$ (accounting for carbon-use efficiency, ϵ).

105 Our specific model for F is:

$$106 \quad F = (1 - \epsilon) \times C \times \frac{V_{max}MB}{k_h + MB} \quad (3)$$

107

108 Following the terminology of Chesson (1998,2012), the above is our “patch” model and our goal
109 is to understand how spatial variances and covariances impact the integrated flux, which
110 represents the spatial expectation or $E[F]$ (hereafter denoted \bar{F}), which represents

$$111 \quad \overline{-C \times (1 - \epsilon) \times \frac{V_{max}MB}{k_h + MB}}.$$

112 The incorrect approach to solving for $E[F]$ is to simply plug-in the mean-field solution:

$$113 \quad \overline{-C} \times \overline{(1 - \epsilon)} \times \frac{\overline{V_{max}} \overline{MB}}{\overline{k_h + MB}} \quad (4)$$

114

115 Analytically, an exact solution would require specification of a joint distribution for C and MB
116 $\pi(MB, C, \theta)$, and solution of the convolution integral:

$$117 \quad \int -f(MB, C, \theta)\pi(MB, C, \theta)dMBdCd\theta \quad (5)$$

118

119 However, following Chesson (2012) and Chakrawal et al. (2019) we are free to approximate the
120 solution for arbitrary distributions using a Taylor Series approximation expanded to the 2nd
121 moment. Specifically, we take the expectation over a multivariable Taylor Series expansion,
122 centered around the mean-field values of all parameters θ (for simplicity, the variables MB and
123 C are included in the parameter vector θ):

$$124 \quad \bar{F} \approx E \left[f(\bar{\theta}) + \frac{1}{2} \theta_{\theta-\bar{\theta}}^T H_{\bar{\theta}} [f(\theta)] \theta_{\theta-\bar{\theta}} \right] \quad (6)$$

125

126 where $H[f(\theta)]$ represents the Hessian matrix of the function that determines the CO_2 efflux F
127 (in this case Michaelis-Menten), $\theta_{\theta-\bar{\theta}}$ represents the deviation from the mean at each instance
128 and for each of the parameters. It can easily be seen that $\theta_{\theta-\bar{\theta}}^T \times \theta_{\theta-\bar{\theta}}$ is the variance-covariance
129 matrix, and that the first moment of the Taylor expansion cancels because the first derivative of
130 $\theta_{\theta-\bar{\theta}}$ is zero.



131 **2.1 Non-dimensionalization**

132 Expanding equation 6 out, we have 5 terms involving the variances of C , MB , $1 - \epsilon$, V_{max} , and
 133 k_h , and 10 terms involving covariances among the parameters. We can redistribute the
 134 expectation operator over this approximation to see that we are dealing with the contributions
 135 from the variance-covariance terms, weighted by the second partial derivatives evaluated at the
 136 mean for each parameter. However, the resulting expression **does not readily yield insight into**
 137 **the impact of scale transition upon the dynamics**, since second partial derivatives and cross
 138 partial derivatives do not have easy intuition. Moreover, variances and covariances depend
 139 arbitrarily upon the scale of units and measurements involved, hindering both intuition and cross-
 140 site comparisons. Therefore, we non-dimensionalize equation 6 for $E[F]$ as follows:

- 141 1) We define a dimensionless quantity λ as $\frac{\overline{MB}}{k_h}$. λ thus represents a multiplicative factor
 142 expressing the ratio of the mean microbial biomass over it's half-saturation value, indicating
 143 the microbial saturation for the decomposition.
 144 2) We divide all of the terms in 6 by their mean-field value, and represent the whole equation
 145 as a product:

146
$$\bar{F} \approx f(\bar{\theta}) + f(\bar{\theta})((\theta - \bar{\theta})^T \frac{\partial^2 f}{\partial \theta^2 \theta = \bar{\theta}} (\theta - \bar{\theta})) = f(\bar{\theta}) \left(1 + \left(\theta - \bar{\theta} \right)^T \frac{\partial^2 f}{\partial \theta^2 \theta = \bar{\theta}} (\theta - \bar{\theta}) \right)$$

147 (7)

- 148 3) We calculate the resulting expression for \bar{F}
 149 4) We notice that $\frac{Var(\theta)}{\bar{\theta}^2}$ can be re-expressed as $(\frac{SD(\theta)}{\bar{\theta}})^2$ which in turn is the square of the
 150 dimensionless coefficient of variation $(CV(\theta))^2$. This enables us to reformulate the
 151 variance terms in (7).
 152 5) Similarly, since the covariance terms can be rewritten as $COV(X, Y) = \rho_{X,Y} SD(X)SD(Y)$,
 153 we have the following equality:

154
$$\frac{COV(X, Y)}{\bar{X}\bar{Y}} = \rho_{X,Y} CV(X)CV(Y) \quad (8)$$

155

156 Applying steps 1-5 to all the terms in the equation, we end up with a fully dimensionless
 157 equation:

158
$$\bar{F} \approx f(\bar{\theta}) \left(1 + \frac{\lambda}{(1+\lambda)^2} [\rho_{k_h, MB} CV(k_h)CV(MB) - CV(MB)^2] + \frac{1}{(1+\lambda)^2} [CV(k_h)^2 - \right.$$

 159
$$\left. \rho_{k_h, MB} CV(h)CV(MB)] + \frac{1}{(1+\lambda)} [\rho_{C, MB} CV(C)CV(MB) + \rho_{V_m, MB} CV(V_m)CV(MB) + \right.$$

 160
$$\left. \rho_{\epsilon, MB} CV(\epsilon)CV(MB) + \rho_{C, k_h} CV(C)CV(k_h) - \rho_{V_m, k_h} CV(V_m)CV(k_h) - \rho_{k_h, \epsilon} CV(k_h)CV(\epsilon)] + \right.$$

 161
$$\left. \rho_{V_m, C} CV(V_m)CV(C) + \rho_{C, \epsilon} CV(C)CV(\epsilon) + \rho_{\epsilon, V_m} CV(\epsilon)CV(V_m) \right) \quad (9)$$

163



164 Note that by symmetry, we have also solved for the case of the forward Michaelis-Menten
 165 kinetics. This can be expressed simply by interchanging C and MB , and by correspondingly
 166 altering λ to represent the ratio of substrate availability over half-saturation.

167 3. Discussion

168 Having fully non-dimensionalized equation 6, we are in a much better position to gain analytical
 169 insight into the scale transition. To begin, we note the pivotal role played by the quantity λ
 170 throughout this equation. λ scales the contributions of the parameter variation and correlation
 171 terms to the deviation from mean field behavior according to the ratios $\frac{\lambda}{(1+\lambda)^2}$, $\frac{1}{(1+\lambda)^2}$, and $\frac{1}{1+\lambda}$. In
 172 particular, all of the parameter variance terms (which have become $CV(\theta)^2$ upon non-
 173 dimensionalization), are scaled by one of these three λ ratios, alongside 7 out of 10 of the
 174 covariance terms. Overall, low λ (here $\lambda < \approx 1$) keeps all of the spatial correction terms in play,
 175 while increasing λ tends to simplify matters. As noted by Sihi et al. (2018), as $MB \rightarrow \infty$
 176 (equivalent to $MB \gg k_h$ or $\lambda \rightarrow \infty$), reverse Michaelis-Menten kinetics converge to first order,
 177 leaving:

$$178 \quad \bar{F} = -C \times (1 - \epsilon) \times V_{max} \quad (10)$$

179 Accordingly, in our setup, the multiplicative factor for the scale transition correction approaches
 180 a simplified expression, as $\lambda \rightarrow \infty$:

$$181 \quad \bar{F} \rightarrow f(\bar{\theta}) \left(1 + \rho_{V_m, C} CV(V_m) CV(C) + \rho_{C, \epsilon} CV(C) CV(\epsilon) + \rho_{\epsilon, V_m} CV(\epsilon) CV(V_m) \right) \quad (11)$$

182 This is actually quite remarkable. Despite invoking the situation where microbial biomass (and
 183 its enzyme supply) is effectively infinite - thus linearizing the underlying patch models - we
 184 cannot eliminate the possibility of a potentially substantial deviation from mean-field when
 185 scaling decomposition kinetics. We note that in this resulting expression, we have reduced the
 186 situation to a set of three critical correlations involving two microbial physiological parameters
 187 (ϵ , and V_m), and substrate availability (C). Regardless of their respective variabilities (CV terms),
 188 if these correlations are close to zero, then the whole expression converges to mean field.

189 Returning to the situation where λ is not large, if we ignore the correlation terms (temporarily
 190 setting to zero), we see that there are direct contributions to the scale transition from the
 191 variability in MB and k_h that may, to some extent, balance each other:

$$192 \quad \bar{F} = f(\bar{\theta}) \left(1 + \frac{1}{(1+\lambda)^2} [CV(k_h)^2] - \frac{\lambda}{(1+\lambda)^2} [CV(MB)^2] \right) \quad (12)$$

193 Focusing on the offsetting correction terms, we can re-write as:

$$194 \quad \frac{\lambda}{(1+\lambda)^2} \left[\frac{CV(k_h)^2}{\lambda} - CV(MB)^2 \right] \quad (13)$$

195

196

197 and for the case of $\lambda = 1$, this becomes:



198
$$\frac{1}{4}[CV(k_h)^2 - CV(MB)^2]$$
 (14)

199

200 Thus, variability in the factors of soil protection that impact upon k_h in practice, can offset the
 201 impact of variability in microbial biomass itself.

202 More generally, starting with our dimensionless equation 9 puts modelers and empiricists in a
 203 better position to assess the quantitative significance of the scale transition correction across
 204 systems compared to expressions with opaque second partial derivatives and cross derivatives,
 205 and arbitrarily scaled variance terms. By re-expressing \bar{F} in terms of dimensionless coefficients
 206 of variation, correlation coefficients and λ , we can plug-in realistic values for variability in any
 207 relevant parameter and assess the % effect on \bar{F} in terms of deviation from mean field behavior.
 208 We argue that this formulation possesses significant advantages not only in understanding how
 209 to scale flux estimates (\bar{F}) *within* a site, but going forward will help facilitate intercomparison
 210 *among* sites in terms of their scale-free variability.

211 3.1 Spatial Colocation of Microbes and Substrate

212 To illustrate these advantages in interpretability, we first take the special case of a model where
 213 we treat all parameters as constant (and known) except substrate and microbial biomass. This
 214 corresponds to setting the other CV and ρ terms to 0. In this case, we are isolating the impact of
 215 the spatial colocation of substrate and decomposers. Our equation becomes:

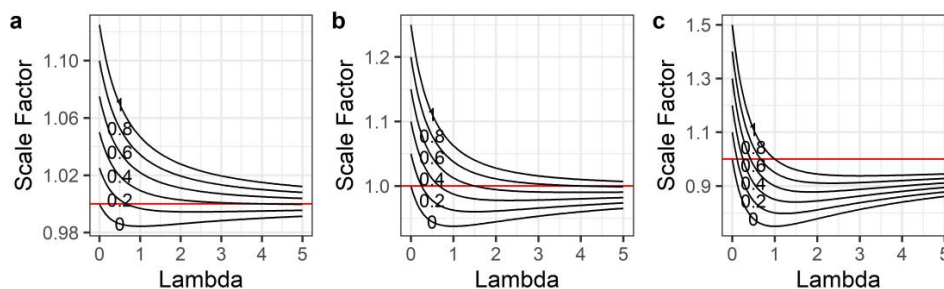
216
$$\bar{F} \approx f(\bar{\theta}) \left(1 - \frac{\lambda}{(1+\lambda)^2} CV(MB)^2 + \frac{1}{(1+\lambda)} (\rho_{C,MB} CV(C) CV(MB)) \right)$$
 (15)

217 In the case of this formulation, there is a very clear dual convergence as λ increases:

- 218 1. deviation from mean-field behavior declines, and
 219 2. first order kinetics are approached

220 Indeed, our equation 15 reveals the exact speed of this convergence in terms of dimensionless λ
 221 and a balance of $CV(MB)$, $CV(C)$ and their correlation.

222 We illustrate the scale transition solutions to equation 15 as a function of lambda for various
 223 choices of $CV(C)$, $CV(MB)$ and ρ :



224



225 *Figure 1: Scale correction factor for models given spatial colocation between microbes and*
226 *substrate across a gradient of λ values, and for a variety of correlation ρ values (0-1), with*
227 *$CV(SOC)$ held constant at 0.5, a) $CV(MB) = 0.25$, b) $CV(MB) = 0.5$, and c) $CV(MB) = 1$.*

228 We see in Fig. 1 that in the case of pure spatial colocation, with no variation in the kinetic
229 parameters, the scale transition correction factor varies from a maximum of 1.5 to a minimum
230 around 0.75, and in all cases indeed converges to 1 as lambda increases. The variability assumed
231 for C and MB impacts only the scale of the correction factor, not the qualitative behavior as λ
232 and ρ vary. One virtue of having a simplified, generic dimensionless equation of this sort is that
233 it enables us to think in a unit-free/scale-free manner about the *plausible* range of the scale
234 transition correction given transparent assumptions about variability and correlations.

235 Another virtue is that it is mathematically tractable to see how the variance and covariance terms
236 can balance each other, and to solve for where they are equal. If we introduce a new term λ_2
237 representing the relationship between $CV(MB)$ and $CV(C)$ as follows $CV(MB) = \lambda_2 CV(C)$, we
238 can re-express the the deviation of the mean-field correction from 1 as:

$$239 \quad CV(MB)^2 \left[\frac{1}{1+\lambda} \left(\rho \lambda_2 - \frac{\lambda}{(1+\lambda)} \right) \right] \quad (16)$$

240 Thus, whether the correction is positive or negative depends crucially on the product of the
241 colocation correlation coefficient ρ and the extent of variability in substrate relative to variability
242 in microbes.

243 If we fix λ_2 to unity, as done in our Fig.1, our mean-field deviation simplifies to:

$$244 \quad CV(MB)^2 \left[\frac{1}{2} \left(\rho \lambda_2 - \frac{1}{2} \right) \right] \quad (17)$$

245 In general, it is clear that the scale transition correction is larger to the extent that microbial
246 variability exceeds substrate variability under reverse michaelis-menten kinetics (the opposite
247 relation holds for forward Michaelis-Menten by symmetry). Thus, variability in microbial
248 biomass is not only important in itself in driving Jensen's Inequality, but also with respect to
249 variability in substrate supply. **Our analysis thus highlights another route of convergence
250 back to the mean field beyond the simple increase of λ : variability in substrate increasing
251 to match variability in microbes in the presence of positive spatial colocation factor.** We
252 also note that the magnitude of the mean field correction scales as the *square* of the coefficient of
253 variation of microbial biomass. Quadratic scaling means that at low to moderate levels of
254 variability, the deviation from mean field behavior is likely to be fairly minimal, but at
255 moderately high to high levels of variability, severe deviations can be expected.

256 3.2 Environmental Heterogeneity

257 So far we have analyzed in depth the role of variability in microbes and their substrate, but not in
258 the ecological drivers underlying maximal reaction rates (i.e. V_{max}) or half-saturation (i.e. k_h).
259 We start with the observation that both linear first order and non-linear microbial models will
260 show characteristic scale transitions given heterogeneity in temperature and soil moisture.
261 Consider the asymptotic convergence of the reverse MM to first order



262
$$\frac{dC}{dt} = -V_{max}\bar{C} \quad (18)$$

263 This is mathematically equivalent to the more standard way of writing these models down as

264
$$\frac{dC}{dt} = -kC \quad (19)$$

265 To make matters clear, we re-express the rate limiting maximal reaction velocity V_{max} first as a
 266 function of temperature (assuming all else constant):

267
$$V_{max} = e^{aT} \quad (20)$$

268 In this case, our integrated flux equation will be:

269
$$\frac{d\bar{C}}{dt} = -e^{aT} \times (1 - \epsilon) \times C \quad (21)$$

 270

271 Allowing for variability in T , this integrated equation will show characteristic scale transitions
 272 given the convex (exponential) relationship with T .

273 Using the Taylor expansion again to second order we have:

274
$$\overline{V_{max}} \approx e^{a\bar{T}} \left(1 + \frac{1}{2} a^2 \text{Var}(T)\right) \quad (22)$$

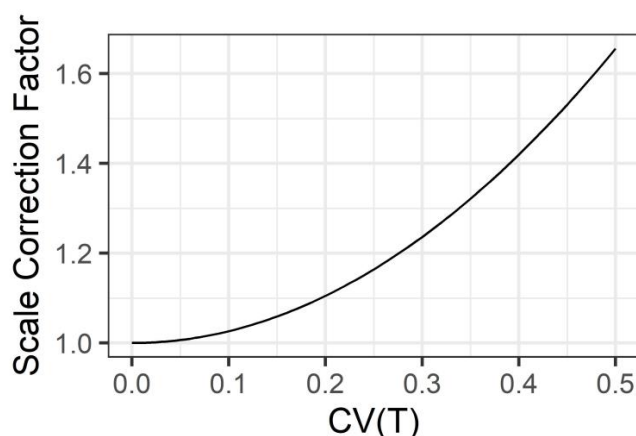
275 The critical scale correction term here is again multiplicative, and we re-express it into a function
 276 of a dimensionless coefficient of variation parameter more suited to ready interpretation. First,
 277 the exponential dependence of respiration on temperature is canonically codified in terms of Q_{10}
 278 scaling. We substitute $a = \frac{\log(Q_{10})}{10}$, and end up with:

279
$$1 + \frac{1}{2} a^2 \text{Var}(T) = 1 + \frac{1}{2} \left(\frac{\log(Q_{10})}{10}\right)^2 \text{Var}(T) = 1 + \frac{1}{200} (\log(Q_{10}))^2 (SD(T))^2 =$$

 280
$$1 + \frac{1}{200} (\log(Q_{10}))^2 (\overline{TCV}(T))^2 \quad (23)$$

 281

282 For a “typical” Q_{10} of 2.5, and a \bar{T} of 25, we see the multiplicative scale transition correction in
 283 figure 2:



284

285 *Figure 2: Scale correction factor for Q10 temperature response scaling given coefficient of*
286 *variation CV(Temp) from 0 to 0.5*

287 As is clear in Fig. 2, the scale transition for temperature is extremely convex. Integration of
288 fluxes over ecosystems with significant heterogeneity in temperature invokes substantial
289 deviation from a mean-field model. For instance, at a CV of 0.2, the scale correction factor is
290 1.10, but by a CV of 0.5 it is 1.66. Obviously, the significance of this depends on the scale and
291 heterogeneity over which an accurate flux model is desired. For a smaller footprint eddy
292 covariance tower (nuria) over a uniform habitat type, soil (and near surface) temperatures
293 probably do not vary by much more than 20%. Regardless, our general mathematical analysis
294 quantifies and clarifies exactly how the scale of variation influences the degree of the scale
295 transition correction.

296 Notably, the only difference between the scale transition correction for first order and for reverse
297 MM kinetics, is that in the latter, there would be additional correlation terms to consider, e.g. the
298 correlation between temperature and V_{max} , temperature and k_h , as well as temperature and C and
299 MB .

300 **3.3 Lessons for Scientific Inference**

301 We close our discussion by considering the implications of the scale transition for advancing the
302 state of biogeochemical modeling. Critically, the representation of non-linear (microbial driven)
303 kinetics is a crucial modeling choice with large implications for long-term SOC forecasts.
304 Traditional first-order PBMs dodge explicit representation of these kinetics, but nonetheless have
305 worked well in practice. This state of affairs persists because both non-linear and linear kinetics
306 are capable of representing coarse-scaled biogeochemistry reasonably well, at least in certain
307 respects. Since first order kinetics are known to be a crude approximation, the crucial question
308 for practice is not whether they are “true”, but rather whether there is significant, systematic
309 information loss inherent to their use. Fortunately, the scale transition offers a clear, clean path to
310 discriminate between these alternative model formulations.



311 As noted throughout, the dimensionless term λ plays a critical role in linking the non-linear
312 (Michaelis-Menten) kinetics to the first order kinetics. As λ increases, the non-linear kinetics
313 converge to first order. Thus, in seeking to infer where the non-linear kinetic models provide
314 substantial advantages, ensuring that λ is not too large ($\gg 1$) is the first priority. Previous work
315 Sihi et al. (2016) has approached this question theoretically, from first principles. Here, we point
316 out that demonstrating substantial deviation from mean-field model when fitting non-linear
317 kinetics to data is both a necessary and sufficient condition for inferring that λ is not too large.
318 Thus we recommend that time series of flux data be fit to both a first order and a non-linear
319 kinetic model, where crucial covariates including substrate (SOC), microbial biomass, and
320 possibly environmental parameters such as temperature, have been measured sufficiently well to
321 quantify the relevant variances and covariances. Where predictive performance and forecasting
322 are the primary goals, we recommend careful consideration of model parameterizations
323 (i.e. based on leave-one-out cross validation), and model combination via “stacking” where it is
324 difficult to infer a decisive “winner” (Yao et al. 2018).

325 In addition to the role of λ , our analysis also clearly shows the contribution of other terms to the
326 scale transition, and thus alternative metrics to assess. First and foremost, accounting for the
327 spatial collocation of microbial biomass and substrate (according to equation 15 above) or the
328 various correlation terms between microbial biomass and kinetic/environmental factors in
329 equation 9. In addition to fitting fully parameterized flux models (as above), simpler statistical
330 models could be fit examining the role of variations in microbial biomass, or collocation of
331 microbial biomass and SOC, in explaining across-site variations in ecosystem respiratory fluxes
332 (F). **A substantial role for either correlation of MB and C, or their variability, would**
333 **constitute ipso facto evidence of the preferability of well-formulated non-linear kinetic**
334 **models.** On the other hand, small roles for collocation, or evidence of large values of λ in practice
335 would suggest minimal advantage to abandoning first order models in favor of more complex
336 microbial models. A meta-analytical approach across sites will benefit greatly from our
337 formulation in terms of dimensionless quantities like λ and the various coefficients of variation.

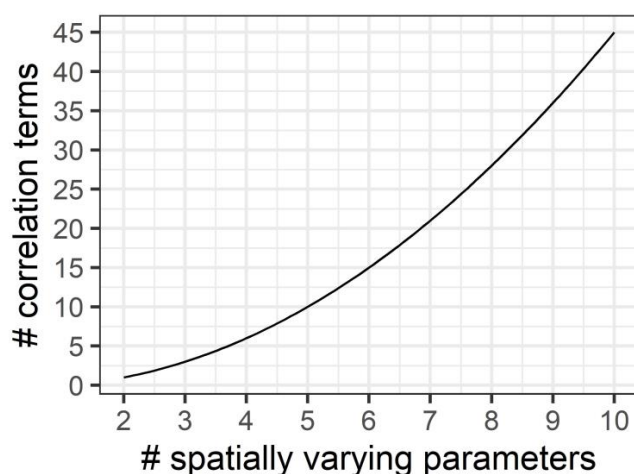
338 4. Conclusions

339 Here, we have illustrated how the spatial scale transition can be expressed in dimensionless form,
340 yielding insight into the systematic operation of Jensen’s Inequality in upscaling microbial
341 decomposition kinetics. Our analysis has identified the central role of the dimensionless quantity
342 λ - representing the ratio of mean-field microbial biomass over its half-saturation value - in
343 governing the extent of the scale transition correction, expressed here in multiplicative form best
344 facilitating comparison among systems. For somewhat simplified scenarios - such as restricting
345 to spatial collocation of substrate and microbes - as $\lambda \rightarrow \infty$, the mean-field correction goes to 0
346 and the model converges to first order.

347 This dual sense of convergence also provides opportunity to empirically test for the presence of
348 significant non-linear microbial dynamics in upscaled field data: to the extent that upscaled
349 fluxes deviate from the flux estimated at mean-field conditions, we have *ipso facto* evidence for
350 the importance of formulating our biogeochemical models with these non-linear terms.
351 Conversely, where there is close agreement between mean-field and upscaled fluxes, there are
352 arguably stronger reasons for retaining first-order process model formulations.



353 In closing, we would like to point out how this mathematical analysis illustrates the challenge of
354 scaling quite nicely. In the context of non-linear models, for each parameter that is allowed to
355 vary in space, there is not only a new variance parameter, but a number of new covariance terms
356 are induced, growing as the factorial of the number of varying parameters $(\frac{5}{2})!$ (Fig. 3). Thus, in
357 the case of the 5 parameter function considered here, the full approximation has 5 mean field
358 terms, 5 coefficients of variation, 10 correlation coefficients, and the dimensionless quantity λ .



359

360 *Figure 3: Model complexity grows exponentially with number of spatially varying parameters.*
361 *We argue to keep models as simple as possible for both analytical and computational*
362 *tractability.*

363 Even with a maximally generic and simplified expression, fitting such non-linear time series
364 models to field data still represents quite a challenge, especially while adequately accounting for
365 and propagating uncertainty. Modelers and theoreticians should appreciate the complexity of the
366 task at hand. Fortunately, our analysis has identified a potentially robust route to limiting model
367 complexity: screen systematically for the importance of various correlations in explaining
368 variations in fluxes. Accordingly, we recommend that research focus first upon spatial collocation
369 of MB and C, which is readily measured, and then to thoughtfully and carefully expand models
370 with additional terms as needed.

371 **Author Contributions:** CHW conceived the original concept, developed the mathematical
372 analysis, and wrote the manuscript. SG developed the concepts, contributed to the mathematical
373 analysis, and co-authored and edited the manuscript.

374 **Competing Interests:** None declared.

375 **Acknowledgements:** We stand on the shoulders of giants: Peter Chesson's research program on
376 Scale Transition was enormously influential. We thank T. Trevor Caughlin for introducing us to
377 Chesson's papers many years ago, and to everyone who has humored discussions of Jensen's
378 Inequality ever since!



379 **References**

- 380 Blankinship, Joseph C., Asmeret Asefaw Berhe, Susan E. Crow, Jennifer L. Druhan, Katherine
381 A. Heckman, Marco Keiluweit, Corey R. Lawrence, et al. 2018. “Improving Understanding of
382 Soil Organic Matter Dynamics by Triangulating Theories, Measurements, and Models.”
383 *Biogeochemistry* 140 (1): 1–13. <https://doi.org/10.1007/s10533-018-0478-2>.
- 384 Blankinship, Joseph C., and Joshua P. Schimel. 2018. “Biotic Versus Abiotic Controls on
385 Bioavailable Soil Organic Carbon.” *Soil Systems* 2 (1): 10.
386 <https://doi.org/10.3390/soilsystems2010010>.
- 387 Chakrawal, Arjun, Anke M Herrmann, Johannes Koestel, Jerker Jarsjö, Naoise Nunan, Thomas
388 Kätterer, and Stefano Manzoni. 2019. “Dynamic Upscaling of Decomposition Kinetics for
389 Carbon Cycling Models.” *Geosci. Model Dev. Discuss. Doi* 10.
- 390 Chesson, Peter. 1998. “Spatial Scales in the Study of Reef Fishes: A Theoretical Perspective.”
391 *Australian Journal of Ecology* 23 (3): 209–15. [https://doi.org/10.1111/j.1442-](https://doi.org/10.1111/j.1442-9993.1998.tb00722.x)
392 [9993.1998.tb00722.x](https://doi.org/10.1111/j.1442-9993.1998.tb00722.x).
- 393 ———. 2009. “Scale Transition Theory with Special Reference to Species Coexistence in a
394 Variable Environment.” *Journal of Biological Dynamics* 3 (2-3): 149–63.
395 <https://doi.org/10.1080/17513750802585491>.
- 396 ———. 2012. “Scale Transition Theory: Its Aims, Motivations and Predictions.” *Ecological*
397 *Complexity*, From spatially explicit population models to mean-field dynamics, 10 (June): 52–68.
398 <https://doi.org/10.1016/j.ecocom.2011.11.002>.
- 399 Georgiou, Katerina, Rose Z. Abramoff, John Harte, William J. Riley, and Margaret S. Torn.
400 2017. “Microbial Community-Level Regulation Explains Soil Carbon Responses to Long-Term
401 Litter Manipulations.” *Nature Communications* 8 (1): 1223. [https://doi.org/10.1038/s41467-017-](https://doi.org/10.1038/s41467-017-01116-z)
402 [01116-z](https://doi.org/10.1038/s41467-017-01116-z).
- 403 Greenland, Sander. 2019. “Valid P-Values Behave Exactly as They Should: Some Misleading
404 Criticisms of P-Values and Their Resolution with S-Values.” *The American Statistician* 73
405 (sup1): 106–14. <https://doi.org/10.1080/00031305.2018.1529625>.
- 406 Levin, Simon A. 1992. “The Problem of Pattern and Scale in Ecology: The Robert H. MacArthur
407 Award Lecture.” *Ecology* 73 (6): 1943–67. <https://doi.org/10.2307/1941447>.
- 408 Parton, W. J., D. S. Schimel, C. V. Cole, and D. S. Ojima. 1987. “Analysis of Factors
409 Controlling Soil Organic Matter Levels in Great Plains Grasslands.” *Soil Science Society of*
410 *America Journal* 51 (5): 1173. <https://doi.org/10.2136/sssaj1987.03615995005100050015x>.
- 411 Ross, Sheldon. 2002. *A First Course in Probability*. Pearson Education India.
- 412 Schimel, Joshua P., and Michael N. Weintraub. 2003. “The Implications of Exoenzyme Activity
413 on Microbial Carbon and Nitrogen Limitation in Soil: A Theoretical Model.” *Soil Biology and*
414 *Biochemistry* 35 (4): 549–63. [https://doi.org/10.1016/S0038-0717\(03\)00015-4](https://doi.org/10.1016/S0038-0717(03)00015-4).



- 415 Sihi, D., S. Gerber, P. W. Inglett, and K. S. Inglett. 2016. “Comparing Models of Microbial–
416 Substrate Interactions and Their Response to Warming.” *Biogeosciences* 13 (6): 1733–52.
417 <https://doi.org/10.5194/bg-13-1733-2016>.
- 418 Todd-Brown, Katherine E. O., Bin Zheng, and Thomas W. Crowther. 2018. “Field-Warmed Soil
419 Carbon Changes Imply High 21st-Century Modeling Uncertainty.” *Biogeosciences* 15 (12):
420 3659–71. <https://doi.org/10.3929/ethz-b-000272804>.
- 421 Van Oijen, Marcel, David Cameron, Peter E. Levy, and Rory Preston. 2017. “Correcting Errors
422 from Spatial Upscaling of Nonlinear Greenhouse Gas Flux Models.” *Environmental Modelling
423 & Software* 94 (August): 157–65. <https://doi.org/10.1016/j.envsoft.2017.03.023>.
- 424 Yao, Y., Vehtari, A., Simpson, D., & Gelman, A. 2018. Using stacking to average Bayesian
425 predictive distributions (with discussion). *Bayesian Analysis*, 13(3), 917-1007.
426
- 427 Wieder, William R., Steven D. Allison, Eric A. Davidson, Katerina Georgiou, Oleksandra
428 Hararuk, Yujie He, Francesca Hopkins, et al. 2015. “Explicitly Representing Soil Microbial
429 Processes in Earth System Models.” *Global Biogeochemical Cycles* 29 (10): 2015GB005188.
430 <https://doi.org/10.1002/2015GB005188>.
- 431 Wieder, William R., Gordon B. Bonan, and Steven D. Allison. 2013. “Global Soil Carbon
432 Projections Are Improved by Modelling Microbial Processes.” *Nature Climate Change* 3 (10):
433 909–12. <https://doi.org/10.1038/nclimate1951>.
- 434 Wieder, William R., Melannie D. Hartman, Benjamin N. Sulman, Ying-Ping Wang, Charles D.
435 Koven, and Gordon B. Bonan. 2018. “Carbon Cycle Confidence and Uncertainty: Exploring
436 Variation Among Soil Biogeochemical Models.” *Global Change Biology* 24 (4): 1563–79.
437 <https://doi.org/10.1111/gcb.13979>.